A 2D SELF–AFFINE ASPERITY MODEL FOR EARTHQUAKE STATISTICS

ORFEO MAZZELLA, FEDERICA MARONE

Abstract. We show that a mathematical model based on fractal fault geometry instead of redistributing local interactions can produce statistics of time and place of earthquake occurence that cannot be discriminated from statistics produced by a SOC model or by a statistical study of empirical earthquakes.

1. Introduction

The evolution of technology and the thickening of geophysical measurements both in time and in space has allowed in the last decades the development of a microseismic study which has become more and more accurate.

The object of research has so moved from a qualitative description of the effects of seismic disasters to a quantitative analysis and interpretation of the experimental data, directed to study the causes and the mechanisms at the real basis of seismic phenomenology.

The theory of Plate Tectonics (Wegener, 1912) according to which the Earth's lithosphere is not static but subdivided into a dozen of main large plates which move relative to each others, together with the previous theory of Elastic Rebound (Reid 1910), by which rocks store elastic energy and deform themselves until a rupture threshold is overpassed, allow the interpretation of tectonic earthquakes as the response of the faults to the accumulating stress due to the slow discontinuous translational tectonic movements. The time scale associated to the duration of the seismic events is orders of magnitude smaller than that one related to the stress accumulation. In this way of reasoning faults are so retained to be those surfaces with a lower resistance, where the propagation of ruptures occurs. Though the simplicity of these basic ideas, that are also well accepted by the whole scientifical community, the much more complex seismic phenomenology presents various not clarified matters of debate.

There are two different main approaches to the study of seismicity, and it is important to distinguish between them for what their goals are concerned. The first is that which

Orfeo Mazzella, Dipartimento di Fisica, Università di Como, I–22100 Como; Institute of Geophysics, ETH–Hönggerberg, CH–8093 Zürich (e–mail: omazzella@ti.com).

Federica Marone, Institute of Geophysics, ETH–Hönggerberg, CH–8093 Zürich (e–mail: federica@tomo.ig.erdw.ethz.ch).

tries to solve local and specifical problems. Many research works take this direction: Das and Kostrov [1] for example have studied the rupture of a simple circular asperity on an infinite fault plane, comprehending the dynamics of the rupture and linking the far–field seismic radiation to the stress drop; Robertson [2] has shown how thickness of wear material developed during brittle faulting increases approximatively linearly with total slip.

The second approach, about which we have centered our study, is that of global models.

This means that we do not focus for example on the generation and propagation of seismic waves, nor on the forces that act over a rock mass or a fault surface. Rather we use the methodology of statistical mechanics to the study of the behavior of macroscopic parameters, dealing in this way with the general properties of the seismic phenomenology and not with the single, particular events.

Many signs of scaling invariance appear in earthquakes phenomena through the presence of power laws. One of the most impressive feature is the Gutenberg–Richter law (GR) [3] for the energy distribution of seismic events. The exponent of this power law is a function of a very important parameter b, the so called *b–value*. The *b–value* has temporal and spatial fluctuations in the interval $[0.5, 1.5]$, and its eventual universality is an important matter of debate since it is not clear if the fluctuations are only statistical, or are on the contrary due to some physical features such as for example the geometical properties of the faults, the physical properties of the medium, or the stress level of the seismic region. Other power laws appear in the distribution of decreasing number of aftershocks in time after a main earthquake (Omori law) [4,5], in the number–size distribution of wear material in fault gouge [6], and in the fractal patterns related to the distribution of epicenters both in space and in time [7]. These are only some of the power laws present in seismic processes.

Theoretical global models insert in this outline and, starting from simplified hypotheses and assumptions, compare their numerical results to the experimental data and to the above mentioned general statistical features, in order to better understand the mechanism involved in the seismic process.

In 1967 Burridge and Knopoff [8] formulated one of the first models in this sense, to simulate the stick–slip phenomenon related to the elastic rebound theory for a fault zone. This model consists of blocks connected by springs, where blocks represent the interacting segments of a fault surface placed on a plane with friction. The blocks are coupled by other springs to a driver which moves with a costant velocity v simulating the slow tectonic motion. Because of the friction, they persist at rest (stick) until the elastic forces overhelm the static friction, resulting in the sliding of one or more blocks (slip). The elongation of the springs corresponds to the accumulating stress, while the sum of the block's slips represents the earthquake energy. This model exhibits the GR law and, under some border conditions, the Omori law.

The Burridge–Knopoff model (BK) is part of a larger class of models: the *Self Organized Criticality* (SOC) class [9]. This class is well represented from the Sandpile model and is

opposed to a second one, that of asperity models. The main hypotheses of SOC models applied to the study of seismicity [10] are that:

- faults are structurally homogeneous. For example in the Carlson–Langer version of the BK model [11], all the blocks have the same mass, the springs are all equal, and the friction does not vary for each site.
- The lithosphere is supposed to be in a Critical Self–Organized state.

The meaning of critical state is the same as in the continuous phase transitions of statistical mechanics. It is in fact a state characterized by spatial and temporal fluctuations on each scale which are the cause of the absence of a characteristic length and time scale of the system, and which give rise to the power laws with universal exponents, i.e. depending only on geometrical and topological features such as the spatial dimension.

In this optics the scaling laws of earthquakes statistics can be directly derived from these power laws intrinsic of such mechanisms.

The consequences of this approach are that a local perturbation can have effects on each scale (long–range of interactions) through a redistribution mechanism, and that there is a lack of a typical dimension of the events.

The meaning of self–organization is that there is not a control parameter (as for example is the temperature for the liquid–gas phase transition). So system tend spontaneously to form the scale invariant structures without any external influence, and the critical point becomes an attractor of the dynamics of the system.

Coherently with the avalanche mechanism of sandpile models, during its whole evolution the lithosphere would have reached a marginally stable state, and now an accumulation of stress in a certain point (an add of grain in sandpile) could infer an earthquake (respectively an avalanche) of each size at each distance, avoiding in this way a local stress accumulation mechanism before a big earthquake. It has been shown [12] that the real origin of self–organized criticality takes place in the mutual interaction between static parameters, representing the slow dynamics in stress accumulation mechanism, and dynamical parameters which describe the fast relaxation earthquake process: seismic events are in fact generated by the lithosphere which has been previously modified by preceding earthquakes and so on in a chain of interacting processes.

Many SOC models have been proposed to study seismicity starting from the BK model, by creating cellular automata [13, 14, 5]. Generally the only power law that they reproduce is the GR law with an universal *b–value* (with the exception [14]). Another property of these model, is that they reveal themselves chaotic and so non–predictable [15].

Opposed to the SOC class, there is the *asperity model* class. These models have hypotheses in strong contraposition with those one of SOC models. Starting from the observation that spatial and temporal distribution of earthquakes and release mechanism seem strickly related to the complexity of fault geometry [16], we show how could the complexity of

the seismic phenomenology entirely and directly be related to the geometrical structural complexity of fault shape. This is in contrast to SOC theory and to BK type models in which the behavior is entirely due to the dynamics of the system. The name of asperity model resumes the following concept which has been applied to eathquakes mechanism by various workers [17, 1]: supposing a fault to be formed by two rough surfaces held together by a compressive normal stress, then such a fault may be expected to consist of separate asperities, and the fracture process leading to an earthquake may be explained as the rupturing of these asperities.

Recent field measurements of the complex geometry of rupture surfaces, from material breakage (μm–scale) to surface rupture of faults (km–scale), indicate that they are best characterized as fractal surfaces [18]. In this perspective rather than being smooth planes, faults would be non–euclidean surfaces of fractal nature, i.e. with irregularities occuring at all scale, as moreover it would have to be expected as seen that faults are the result of a fracture in an inhomogeneous medium.

Fractals provide a good characterization of those shapes highly irregular and complex but that present the same degree of complexity at each magnification they are observed. This phenomenon is called scale–invariance and is strickly characterized by the absence of a characteristic length, by the presence of power laws, and comes from the iteration of non–linear dynamical systems [19]. Our intention is then to show if it is possible to find some analogies between the scaling laws intrinsic in the definition of fractals and those ones typical of experimental earthquakes phenomenology.

The *Self–affine Asperity Model* (SAM) [20,21] is in this sense a fractal asperity model with global properties, and is one of the most significant example of how the power laws of earthquakes statistics can be directly derived from the power laws intrinsically present in the scaling of surface topography, without making use of SOC theory. In particular the one–dimensional version (1D SAM) is a geometric model which intends to mimic fault dynamics by simulating sliding of two self–affine fractional Brownian profiles (fBm) one over the other. The fBms are the 1D representation of the two opposite fractal surfaces of a transform fault, for example, in motion relative one to another and are composed by a sequence of asperities at each characteristic length. An earthquake is then a sudden rupture resulting from the collision of two asperities because of the sliding mechanism, and the epicenter is the point where the rupture begins.

For sake of simplicity, in a first version of 1D SAM model, it has been supposed that the asperities did not break but can overlap with respect to each others, and that the energy of a seismic event is proportional to the linear dimensions of the colliding asperities. Thanks to its simplicity, this model has been studied both numerically and analytically [20, 21], through the mathematical properties of fBms, exhibiting many general features of the earthquakes statistics. In particular it has reproduced the GR law relating the *b–value* to the roughness of the faults through the Hurst parameter by an analytical relationship. The exponent b would be in this way not universal, besides suggesting the idea of temporal variations of its value with the age of the fault, since it seems natural to expect that the

roughness of a fault decreases in geological times. The model exhibits also the fractal spatial distribution of epicenters, relating this property to a finite size effect of the fault dimensions in an analytical way. It reproduces then the $1/f$ noise, starting from the analysis of the released energy signal in time; this means that a synthetic seismic event may be influenced by another one very distant in time because of the absence of a maximum autocorrelation time. The model reveals properties of strong nonlocality in space too: an event with a certain epicenter at a certain time can trigger a successive event also at great distances.

SAM models contrast to SOC models in some fundamental and basic assumptions. SAM approach shows how the concept of fractal geometrical complexity (not taken into account for SOC models) can potentially tie the scaling of surface topography to that of earthquake processes without making use of SOC theory, nor of dynamical complexity.

In SAM perspective the local accumulation of pressure is at the very origin of the seismic events, and there is no more interplay between the earthquakes and the fault general structural properties: while in SOC models earthquakes are integrating part of the generation and evolution phenomena of the fault structure, for SAM the creation of the fault is distinguished from its evolution and plays the dominant role since all the informations of the future earthquakes statistics are contained in it through the choice of a starting roughness parameter H which resumes the general fault properties. The idea is that the time scale of lithospheric processes (rearrangement's geological times of the lithosphere) exceeed the time scale of human measurements, and earthquakes do not modify the general properties of fault geometry. Moreover, the overlapping version of the SAM model above discussed diametrically opposes to the SOC perspective since faults shapes are not at all modified from seismic events, turning SAM model in a sort of limit of infinity rigidity of BK models. Obviously this version can be considered as a provocation to SOC theory, or better as a hint to be conscious that more realistic situations could well correspond to intermediate cases where both the geometrical and dynamical complexities could play a principal role.

A refinement of the SAM model which could account for a local description of the seismic phenomenology, by means of a breaking mechanism of the colliding asperities, has been proposed [21] to study the temporal distribution of aftershocks: the aftershocks are in fact those seismic events with a lower intensity which follow a main shock, and are intrinsically linked to the structural situation locally existing after that main shock.

Operatively, in our numerical simulations, a fracture process propagates from the epicenter and breaks the smallest asperity, assuming the energy of the earthquake to be proportional to the linear dimension of the fracture. This generalization of the model, a part from being more realistic, exhibits the Omori law.

In this paper we improve the last version of SAM model with breaking mechanism, studying completely its derived earthquakes statistics, beyond the Omori law previously reproduced. The refined model in fact exhibits, in addition to the GR law and to the fractal distribution of epicenters, the fractal distribution of broken asperities in fault gouge. Interesting results come also from the study of the space–time distribution of earthquakes, which shows

evidence of the migration of seismic events. The last result will be compared to some experimental measurements [22]. Results of the 1D SAM model are however in some case still too simple to compare to observed earthquake statistics due both to the 2D nature of real fault surfaces and to the trivial dynamics used. We have seek to remedy to this deficiency by extending the 1D to 2D SAM, with fractional Brownian surfaces sliding one over the other, and by simulating stick–slip mechanism through a more complex dynamics.

In the 2D SAM model we have focused our attention in the GR law. The main result is that the *b–value*, a part from being dependent from the roughness of the fault as in the 1D case, depends on the dimensions of the fault surfaces. There are also two different exponents, one for small and one for large earthquakes energies, inferred from the characteristic dimensions of the fault area, according to some studies [23] and resembling the experimental evidence. These results strengthen the previous ones against the concept of universality of the *b–value*.

We have then studied the distribution of hypocenters and we have found that they comprise a spatial fractal set with a fractal dimension which tends to two for the number of events tending to infinity (homogeneous filled space in discretized case). Instead the temporal set gives an exponent of one indicating uniformly random distribution. As for the 1D case, we have in the end generalized to 2D the study of the space–time distribution of hypocenters to evidence the migration of the events. Whenever possible the numerical results are compared to the analytical and to the experimental ones.

The outline of the paper is the following. In section 2 we define the 1D model which includes the effect of the breaking of the asperities, we recall some mathematical properties of the self–affine profiles and we study the resulting earthquakes statistics. In section 3 we introduce the extension to 2D of the SAM model and we show the relative results. Section 4 is dedicated to the conclusions.

2. 1D SAM Model with Breaking Mechanism

In this section we study the simplified one–dimensional Self–Affine Asperity Model (1D SAM) to mimics the dynamics of a fault.

The previous version of 1D SAM model [20] assumed that the faults were infinitely rigid fractal objects not at all modified by the seismic activity.

Here we improve the basic model in order to include a local rearrangement of the Earth crust as a consequence of the occurrence of an earthquake, considering the asperity breaking in the collision [21], and therefore including a geometric change of the fault profiles in the numerical simulations.

Let we start dealing with the most important general ideas and properties of this model. Already in the last centuries the importance of the surface roughness in friction was recognized. Friction is caused by the interaction of asperities and since it is a contact property, it is likely sensitive to the topography of the surfaces.

An asperity is defined as a region of exceptionally high moment release and hence a region in which the stress drop is much greater than the surroundings regions on the fault. Asperities are simply sites of higher than usual frictional resistance either because of higher effective normal stress or because they have not slipped in an earthquake for a long time [24]. Being faults regions very resistent with respect to the surrounding ones, asperities are then less inclined to slip when subjected to shear stress [25].

In this outline, the clue idea of asperity models is that fault topography is constituted by a distribution of asperities of different dimension and resistence, and that an earthquake of large intensity correspond to the breaking of a single large asperity or equivalently of many smaller asperities [26].

Several researchers [18] made a general study of the topography of rock surfaces and found that natural rock surfaces resembled fractional Brownian surfaces. Because of our simplified 1D SAM version, we work with topographic traces of the fault, simulated by random signals, in particular fractional Brownian motion (fBm) [27]. A fractional Brownian motion is a random process with a position function $X_H(x)$. Its increments

$$\Delta X_H(\Delta x) = X_H(x_2) - X_H(x_1)$$

have a Gaussian distribution with variance following a power law distribution

$$< \Delta {X_H}^2(\Delta x) > \propto \ \Delta x^{2H}$$

where $\Delta x = |x_2 - x_1|$ and the angular brackets denote averages over many samples of $X_H(x)$.

This function is stationary, meaning that its mean square increments depend only of the incremental distance Δx, and also isotropic, signifying that all x's are statistically equivalent. Furthermore such a trace is characterized by the parameter H, called the *Hurst parameter* [28], which controls its roughness and has a value $0 \leq H \leq 1$. The fractal dimension of the graph associated at such a trace is $D = 2 - H$, while a differentiable curve corresponds to $H = 1$. In particular the case $H = 0.5$ represents the ordinary Brownian motion with totally independent increments. This means that in the formation of the inhomogeneities the accumulation of the anomalies is a totally random, memoryless process. The case $H < 0.5$ has negatively correlated increments. This means that there is a tendency of changing the function in the opposite direction to the former step. The 1D trace looks therefore sharp and jagged. The case $H > 0.5$ has positively correlated increments: there is a persistency process, future movements tend to be in the same direction as former step. The curve therefore looks smoother, gradients between neighboring points are much less steep than in the previous case.

The $X_H(x)$ traces are characterized by a non–uniform scaling and hence are self–affine objects: if the distance scale Δx is changed by a factor r, then the increments ΔX_H change by a factor r^H.

Following the empirical finding that roughness of faults could be characterized as fractional Brownian surfaces with Hurst factor in the range 0.3–0.8 [18], for sake of simplicity we based our 1D numerical simulations on the interaction of two Brownian profiles with $H = 0.5$. To generate a trace of fBm, many algorithms [27,29] exist. For the simple case of the random walk ($H = 0.5$) a trace can be created through the sum of random variables $\{x_i\}$ uniformely distributed:

$$X_{1/2}(j) = \sum_{i=1}^{j} x_i \quad \text{with } j = 1, 2, \ldots, L.$$

The random variables can be generated according to the following algorithm:

$$x_i = \begin{cases} 1 & p_1 = 1/3 \\ 0 & p_2 = 1/3 \\ -1 & p_3 = 1/3 \end{cases} \qquad \forall i \in [1, L].$$

The 1D SAM model is defined by the following dynamical rules:

(i) We generate, at the synthetic time $t = 0$, two profiles, $X^{\inf}_{1/2}(j)$ and $X^{\sup}_{1/2}(j)$, with $j = 1, 2, \ldots, L$. In our numerical simulations we have chosen $L = 10000$.

(ii) The initial condition is obtained by translating the superior profile until contact is reached in the point where the heights difference is minimal:

$$X^{\sup}_{1/2}(j) = {}^{\text{old}}X^{\sup}_{1/2}(j) + \max_{i\in[1,L]}\{X^{\inf}_{1/2}(i) - {}^{\text{old}}X^{\sup}_{1/2}(i)\}.$$

This action simulates a force normal to the fault, which tends to press it.

(iii) The successive evolution is obtained by translating the superior profile of one unit in a parallel way with respect to the other one in the negative sense of j–axis, at a constant speed, when the time progresses from t to $t + 1$.

For $t^* \in \aleph$ with $t^* \geq 0$

$$\begin{aligned} X^{\sup}_{1/2}(j)_{t=t^*} &= X^{\sup}_{1/2}(j + t^*)_{t=0} \\ X^{\inf}_{1/2}(j)_{t=t^*} &= X^{\inf}_{1/2}(j)_{t=0} \end{aligned} \quad \text{with } j = 1, 2, \ldots, L - t^*.$$

(iv) When there is a collision between two asperities and the translational motion is impeded, an earthquake occurs, the smallest asperity breaks and the old profile is substituted by a new fBm with the same Hurst parameter H, which starts in the point of collision and stops when the new trace crosses the old one (see figure 1), or when the bounds of the fault are reached in the sites $j = 1$ or $j = L$.

(v) After every sliding step and before the next one, at the site $j = L$ of the superior profile a new point is created, so that interaction can occur along the whole fault. Moreover every time the two profiles are put in contact, i.e. rules are restarted and

reiterated from point (ii). The algorithm is stopped when $N = 10000$ synthetic earthquakes are generated.

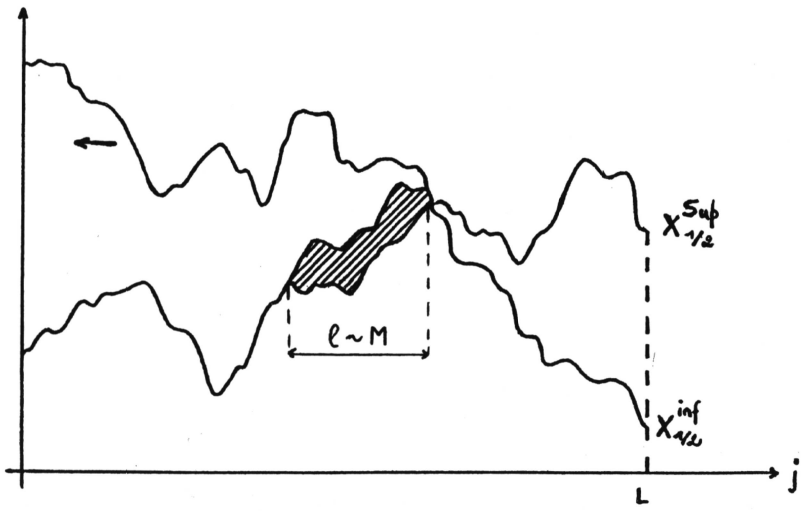

FIGURE 1. Example of asperity rupture.

In this procedure we made use of the following definitions:

(i) The energy or equivalently the seismic moment released by the earthquake is defined as the linear length of the broken asperity.
(ii) The epicenter of the earthquake is that point where the rupture of the asperity begins.

In this model, the region between the two sliding profiles is empty. This assumption is consistent with a configuration of space between two fault surfaces (*fault gouge*) filled with fragmentated material, which organizes itself in such a way that it acts like roller bearings [30]. The existence of so a region between the two rough surfaces could then be related to the so–called seismic gap, namely an extended area where two tectonic plates can creep on each other without producing the amount of heat expected from usual friction forces. This zone slides and has no influences on the dynamics due to its relatively lower viscosity.

The explicit introduction of the fault geometry in a model for seismicity was already been supposed by Huang and Turcotte [31]. Unlike the SAM model, which describes the seismic activity considering two profiles sliding one over the other, they introduced a static model where the average of all seismic events is taken on many uncorrelated realizations of one single fractal profile. The SAM model with breaking mechanism corresponds to an intermediate case between SOC models, where earthquakes are an integrating part of the generation and evolution of the fault structure and the first simplified version of 1D SAM model, where earthquake dynamics had no local effect on the structure of the profile. This

extended model represents in fact a more reasonable situation with earthquakes locally changing the shape of the fault.

From these rules we have easily derived a synthetic earthquake statistics. In particular we studied the Gutenberg–Richter law, the distribution of epicenters both in space and time and the size distribution of the broken asperities.

2.1. **Gutenberg–Richter law.**

On the basis of thousands of earthquake readings Gutenberg and Richter [3] established in 1956 a relationship for the seismic moment distribution, today known as *Gutenberg–Richter (GR) law*:

$$N_{\text{cum}}(M) = aM^{-b/c} \propto M^{-B} \tag{1}$$

where a is an empirical parameter, b is the famous *b–value* before mentioned, $B = b/c$ with $c = 1.5$ [32] and $N_{\text{cum}}(M)$ is the number of earthquakes per unit of time with a seismic moment greater than M. This relationship can be applied both for global and for local earthquakes, but does not appear to characterize seismicity on individual faults [33] nor for earthquake populations with magnitudes less than 3 [34]. As about for the parameters, a is variable in time and in space and it is a value for the regional seismicity, while the *b–value* is generally in the range $0.5 < b < 1.5$ [35] depending on the Earth region considered. The last might depend on three factors: (1) the geometrical properties of the fault [20, 21, 31], (2) the physical properties of the medium [36] and (3) the stress level of the seismic region [31, 37]. The numerical simulations with fBms characterized by $H = 0.5$ provide a clear evidence that our model exhibits a power law directly coming from the scaling relations intrinsically present in the fault shapes and from the previous definition of seismic moment. This power law represents in the SAM model perspective the GR law. In figure 2 is presented the non cumulative distribution:

$$N(M) \propto M^{-B-1}$$

referred to a $300'000$ earthquakes set with $B = 0.954 \pm 0.020$. Referring to (1), this value corresponds to $b \approx 1.431 \pm 0.030$ which falls in the interval of experimentally observed values.

There is an evidence of a deviation from a theoretical line for events with small and big seismic moment. Because of the high probability to intersect and break only the extremities of the asperities, when the two fBms are geometrically put in contact, we in fact obtain more small earthquakes than the GR law predicts. This configuration corresponds to a condition with weak normal forces which do not allow the two opposite fault segments to reach an appreciable contact surface. Laboratory results on rock friction [38] show that the real contact area between to rough surfaces at a confining pressure of 1/2 kbar is as small as a few percent of the total surfaces area. This threshold is not reached in SAM model since the contact routine almost often implies contact in only a single point of the fault.

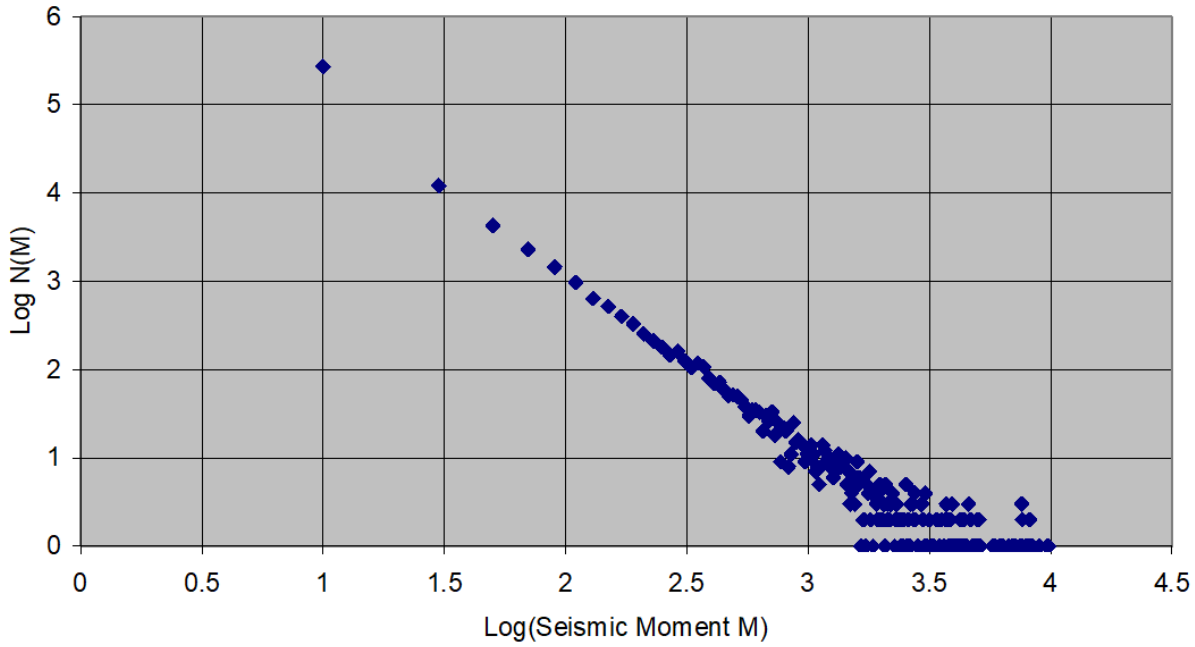

FIGURE 2. Non cumulative Gutenberg–Richter law from 1D SAM model.

About large seismic moment synthetic earthquakes, the dispertion for these events is an effect of the finite size of the fault. In fact there is a superior limit of the seismic moment [11], which is determined by the earthquakes that interest the whole length of the fault: $M_{\max} = L$. The parameter B linked to the *b–value* can also be derived analytically.

Consider two traces of fBm of infinite length, X_H^1 and X_H^2, characterized by the same Hurst parameter H, and with the same starting point position $X_H^1(0) = X_H^2(0)$ as showed in figure 3.

The intersection set is $X_H^1 \cap X_H^2 = \{I_0, I_1, I_2, \ldots\}$. Each portion of the plane in figure with $j \in [j_{I_k}, j_{I_{k+1}}]$ and $k \in \aleph$ is representative of the rupture of an asperity at a certain time t_k: a rupture is in fact a fBm starting from a point at the same height of the asperity profile, the epicenter, and propagating until it intersects the asperity profile in a new point.

The shaded area between X_H^1 and X_H^2 for $j \in [j_{I_k}, j_{I_{k+1}}]$ then represents the surface of the broken asperity in the k–earthquake.

Observing that the difference between X_H^1 and X_H^2 is a self–affine trace too with the same Hurst parameter, we consider the profile:

$$W_H(j) = X_H^1(j) - X_H^2(j) \qquad \text{with } j \geq 0.$$

The seismic moment distribution is by definition simply the length of the "gaps" between the points obtained intersecting $W_H(j)$ with a straight horizontal line at zero height.

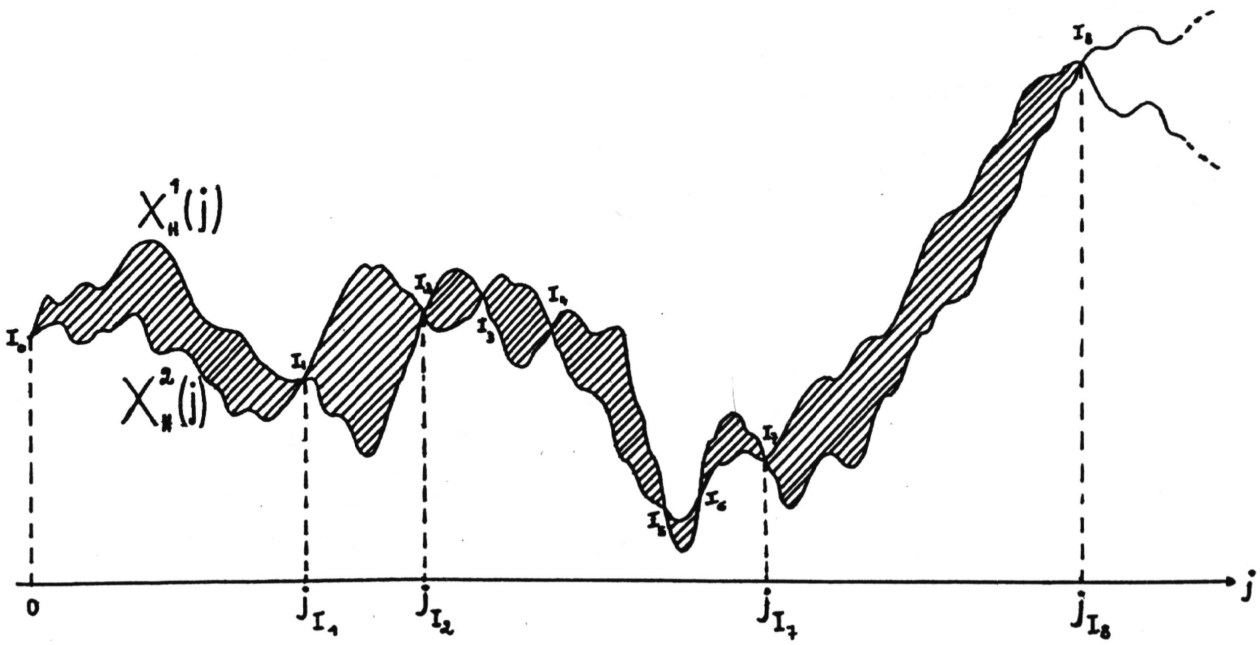

FIGURE 3. Example of fBm traces with same starting point.

If we consider a fractional Brownian object, embedded in a d–dimensional Euclidean, space having a fractal dimension $D = d - H$, its intersection with an hyperplane of dimension $d - 1$ will be an ensemble of dimension:

$$D = (d - H) + (d - 1) - d = d - H - 1.$$

In the 1D SAM configuration $d = 2$ and the set obtained intersecting $W_H(j)$ with a straight line has a fractal dimension $D = 1 - H$. The number of gaps greater than l between these intersection points is therefore given by [19]:

$$N_{\text{cum}}(l) = L \cdot l^{-D} = L \cdot l^{H-1}$$

where L is a constant called *lacunarity*. According to the SAM definition of seismic moment, and by comparing this equation with (1), one gets the relationship between the exponent B of the Gutenberg–Richter law and the Hurst exponent which accounts for the fractal properties of the faults:

$$B = 1 - H.$$

This dependence between B (and consequently the *b–value*) and the roughness can be simply interpreted. The smaller H, the more rough the surfaces are; this means that there are many small asperities and so the statistics is dominated by earthquakes with a low energy and B has a large value. As a consequence of this simple argumentation, by supposing that the effect of the fault slipping is a smoothing of the profiles, i.e. an increase of H, one could guess that the older the fault profile, the smaller the *b–value*.

This result is in contrast with the universality of the *b–value* stated from SOC models: in our interpretation the fluctuations of the B exponent are not only statistical but are on the contrary due to the structural and geometrical variations of the different faults.

For our profiles with $H = 0.5$ we should obtain $B = 0.5$. We can interpret this analytical result as an inferior limit. In fact the asperity is a particular segment of a fBm, characterized by an inversion point, i.e. it contains a maximum or a minimum in its neighbourhood, and this information is missing in figure 3 (see for example $j \in [j_{I_7}, j_{I_8}]$) and in its relative argumentation.

In the numerical simulation the fracture has in this way a greater probability of intersecting, in a lower number of steps, the profile of the asperity to be broken with respect to the analytical discussion.

Second, the numerical algorithm fixes a minimum and a maximum spatial bounds in the sites $j = 0$ and $j = L$ which automatically limit the enlargement of those earthquakes whose ruptures would exceed these bounds.

Both these properties contribute to overestimate those earthquakes with small energies and, as a consequence, the numerical set of zeros of $W_H(j)$ has a greater fractal dimension D with respect to that based on the analytical derivation. As a result the parameter B obtained from the numerical simulations, $B = 0.954 \pm 0.020$, is greater than the analytical one.

2.2. **Wear material distribution.**

The brittle failure of rock in faults caused by frictional sliding and erosion produces fractured material known as cataclastic rock or breccia. At shallow depths in the Earth's crust, this material is non cohesive and is called *fault gouge*.

The comminution model of fragmentation is a way of describing this process and is based on the hypothesis that direct contact between two fragments of wear equal size during the fragmentation process will result in the break up of one of the blocks. It is unlikely that small fragments will break large fragments or vice versa [6, 39].

According to this model, both from laboratory experiments and natural fault gouge observation, it has been found that comminution produces a fractal size distribution of grains. The fragmentation process is so characterized by self–similarity through the power law :

$$N(V) \sim V^{-D} \tag{2}$$

where $N(V)$ is the number of fragments, i.e. broken asperities in SAM perspective, with volume V.

Due to our simplification to 1D traces, we study the 2D–area of the broken asperities instead of the volume, and the fractal dimension of the power law consequently reduces to $D_{2D} = D_{3D} - 1$ [19].

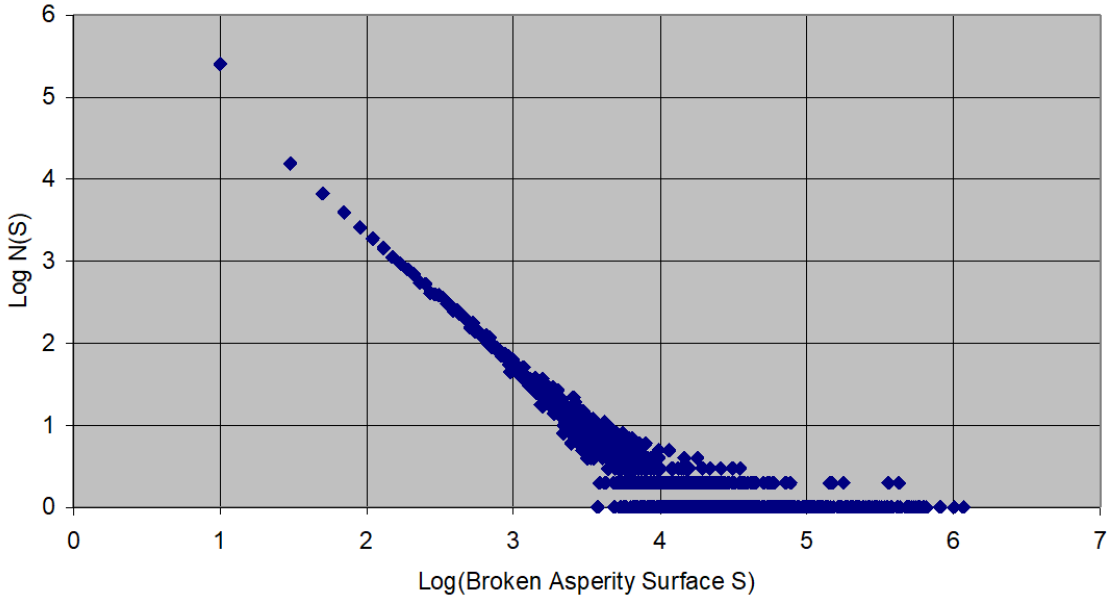

Figure 4. Wear material distribution from 1D SAM model.

The results of the numerical simulations, with $H = 0.5$ and $L = N = 10000$, agree with (2). We in fact obtain a power law behavior with an average fractal dimension of 1.600 ± 0.013 corresponding to a fractal dimension of 2.600 ± 0.013 in the 3D real case (see figure 4).

This is in perfect agreement with laboratory experiments [40] and with the data observed in nature for the Lopez Fault, which gives a fractal dimension of 2.60 ± 0.11 [6, 39].

2.3. **Space–time distribution of epicenters.**

Apart from a non–random component which in most cases can be explained by aftershocks [41, 4, 5], randomness seems to dominate the occurrence of earthquakes avoiding appreciable results in the investigation of seismic cycles. However, the study of two–dimensional graphs in which the location of earthquakes is considered in addition to the time of occurrence, shows different and interesting characteristics. Since earthquakes tend to occur as roughly linear belts along the Earth's surface, the spatial coordinate which specifies the location of events in such these graphs can be chosen as the distance along these seismogenic structures. A belt can be in fact approximated as a line defined by segments of great circles on which earthquakes epicenters, within a specified distance, can be perpendicularly projected.

Several researchers have observed that large earthquakes migrate along seismic belts as time progresses [22, 42]. In order to analyse this aspect for our model, we studied the space–time distribution of the epicenters. In this case a seismic event is simultaneously

characterized by the spatial coordinate in the j–axis, which locates the synthetic epicenter on the fault, and by the temporal coordinate t, which accounts for the progressing of synthetic time.

In figure 5a the results for a fault segment of a numerical simulation sample with $H = 0.5$ and $L = N = 10000$ are shown.

The migration of the epicenters is clearly visible in form of oblique lines representing sequences of points propagating in the negative sense of the spatial j–axis, i.e. in the direction of the translating motion of the superior fBm. A sequence of neighbouring points on these imaginary lines, is therefore representative of a configuration with a large asperity, belonging to te superior fault segment, which moves with a constant velocity and crashes repeatedly through smaller opposite asperities until it breaks itself because of the collision with a larger asperity, or until it reaches the fault bound in the site $j = 0$. Since the translating mechanism works at a velocity of one spatial unit at each temporal unit, and since these units have the same lengths, observe that coherently the pendence of these straight lines in the graph reported is $m = -1$.

Comparing our results with the data referred to a fault in South America [22] (figure 5b), we found a good apparent quality correlation between our results and experimental ones. Though this apparent analogy, there are fundamental differences between the two results: in our approach the migration of events is in fact referred to the very slow relative translational motion of the asperities and consequently of the fault (of the order of tens cm/yr), while in the other approach the triggering of subsequent earthquakes is due to a mechanism of deformation front propagation at velocities of about 100 km/yr. Scholz also hypothizes that the additional stress due to the front must be tensorially additive to the preexisting stress to trigger a new seismic event, and that the sequence of recognizable earthquakes can propagate at speed near the shear velocity [43].

The same work has also been done for the previous overlapping 1D SAM model, where there was not any break of asperity (figure 6, with time in x–axis and space in y–axis). In this case the points are excessively correlated compared to the previous figure 5a. This is justified, because the big asperities, which do not break as the faulting process progresses, continue to cause earthquakes along the fault.

2.4. **Spatial distribution of epicenters.**

Many authors pointed out that the epicenters tend to cover a fractal set with a fractal dimension which is a high irregular function of space and time [7]. One of the most interesting feature is represented by the evidence that the spatial distribution of the epicenters along a linear seismogenic structure seems to exhibits self–similar properties.

Thanks to the simple dynamics of the SAM model, we can simply study the spatial distribution of the epicenters.

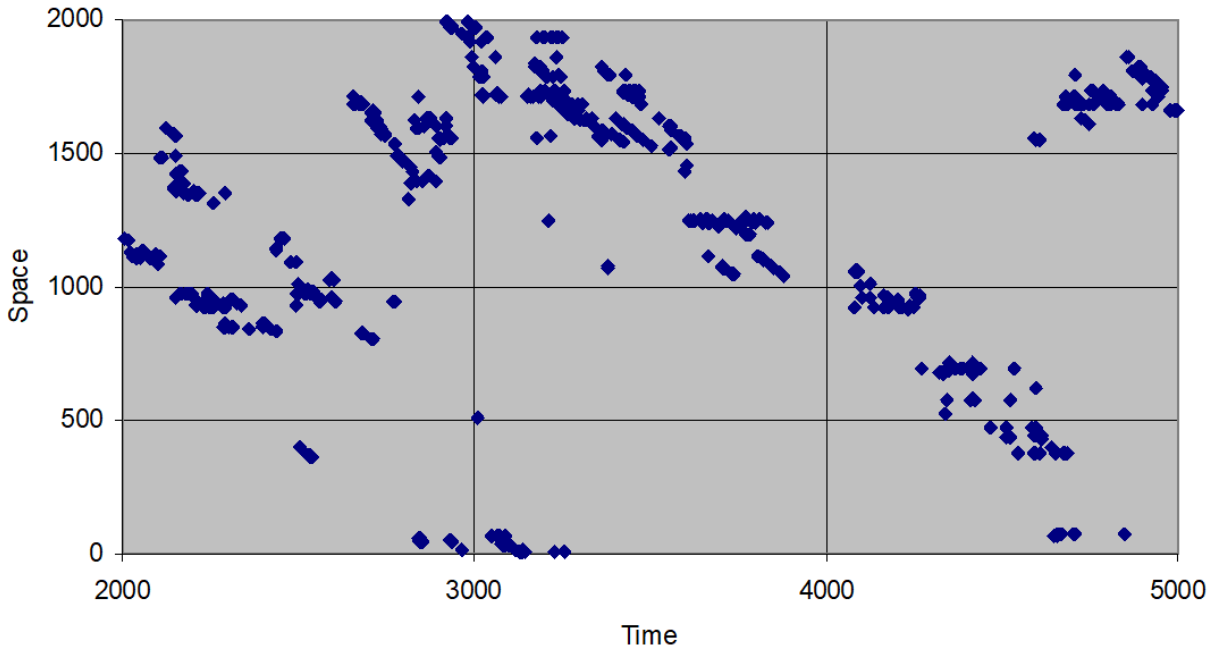

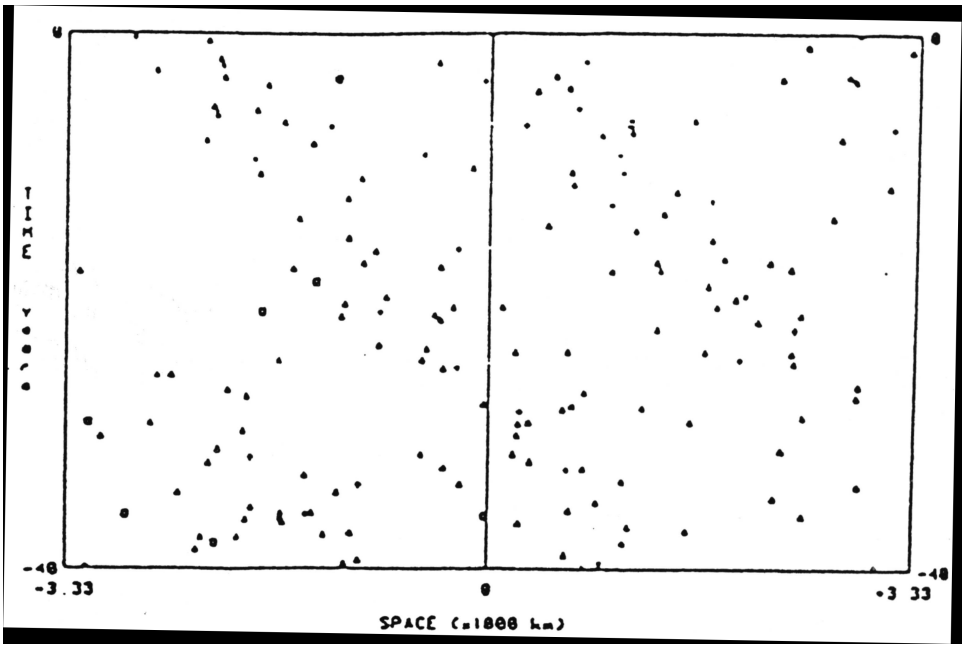

Figure 5. (a) 1D SAM results for the space–time distribution of epicenters; (b) space–time distribution of earthquakes with magnitudo greater than 7.7 occurred in fourthy years along a south–american seismogenetic structure.

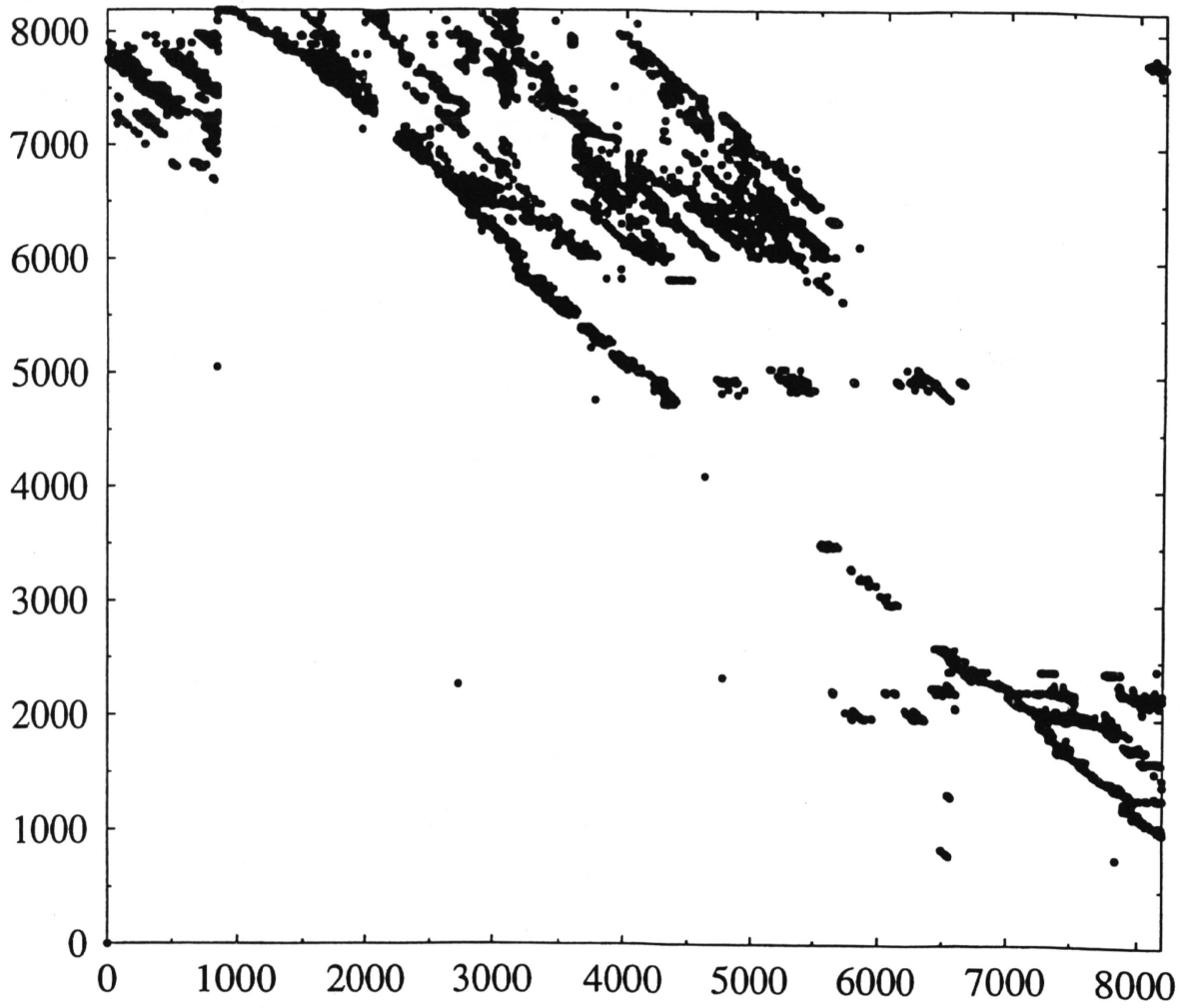

Figure 6. Overlapping 1D SAM results for the space–time distribution of epicenters.

We studied in particular the fractal dimension of the spatial distribution of epicenters in relationship with the flowing of synthetic time for samples with $H = 0.5$ and $L = 10000$ fixed. With the time increasing, the earthquakes number N enlarges and the spatial fractal dimension D_S of the epicenter set tends to 1 (compact set of epicenters). We have in particular studied three earthquakes set configurations with $N = 2500, 6250, 10000$ obtaining respectively values for $D_S = 0.75, 0.83, 0.95$ through the box–counting method. These values are similar to those obtained in the more simplified overlapping 1D SAM model studied for different H and L parameters [21, 44]. The dependence between D_S and N is intuitive: if the fault profiles could slip for an infinite time, each point of the inferior profile could be, theoretically, an epicenter because it, sooner or later, would be hit by an asperity of the superior fault profile.

3. 2D SAM Extension

In the previous section for sake of simplicity we have limited ourselves to the 1D case of faults profiles interacting by means of a simplified dynamics. The study of seismic events in time has taken in our approach a back seat: we have not introduced either any definition of quiescence time or a stick–slip mechanism, and on the contrary we have supposed the fault profiles to slide with a constant velocity. Our attention has been in fact more focused on the statistics of seismic quantities such as energy, epicenter, and wear material size, often leaving their temporal placement out of consideration. Temporal study of events from 1D SAM model however has not been neglected at all and, though the trivial dynamics, it has been carried out in the space–time distribution of epicenters previously seen (figure 5a), and in the $1/f$ noise and Omori law, respectively for the temporal correlation of earthquakes and for the distribution of aftershocks in time [21].

At this point it seems a natural evolution to improve and extend the 1D to 2D SAM model intending to mimic a more realistic and complex fault dynamics by simulating sliding of two fractal surfaces one over the other and comprehending a stick–slip mechanism.

The mathematical tool that allows us to extend the shape of the faults to an higher dimension is the fractional Brownian (fB) surface, a generalization of self–affine traces of fBm in 2D [27]. The single variable x in a fBm can be in fact replaced by coordinates x and y in the plane to give $S_H(x, y)$ as the surface altitude at position (x, y) as shown for one example of $H = 0.5$ in figure 7 for the discretized case. A fB surface is generated by a self–affine stochastic process whose increments have a Gaussian distribution with variance following the power law close in analogy to the 1D case:

$$< \Delta S_H^2(\Delta r) > \propto \Delta r^H$$

where $\Delta r^2 = \Delta x^2 + \Delta y^2$ and the angular brackets denote averages over many samples of $S_H(x, y)$. The graph associated to such a surface has a fractal dimension $D = 3 - H$ and it is characterized by the Hurst parameter H which controls its roughness: $H = 0$ yields a white noise surface, while $H = 1$, a plane.

Some studies have evidenced an existent anisotropy in the topography between the more jagged profiles taken perpendicular to the slip vector and the smoother profiles taken parallel to it [45]. Our choice of simulating the fault shape through fB surfaces neglect this property because of their isotropy in the roughness. The intersection of each vertical plane with the surface $S_H(x, y)$ is in fact a self–affine fBm trace characterized by H and has a fractal dimension one less than the surface itself $D_{\text{trace}} = D_{\text{surface}} - 1 = 2 - H$ [19].

The algorithm used to construct fB surfaces takes advantage of the Fourier filtering method to obtain a random function with a spectral density in the desired power law form , whose exponent is directly linked to H [29].

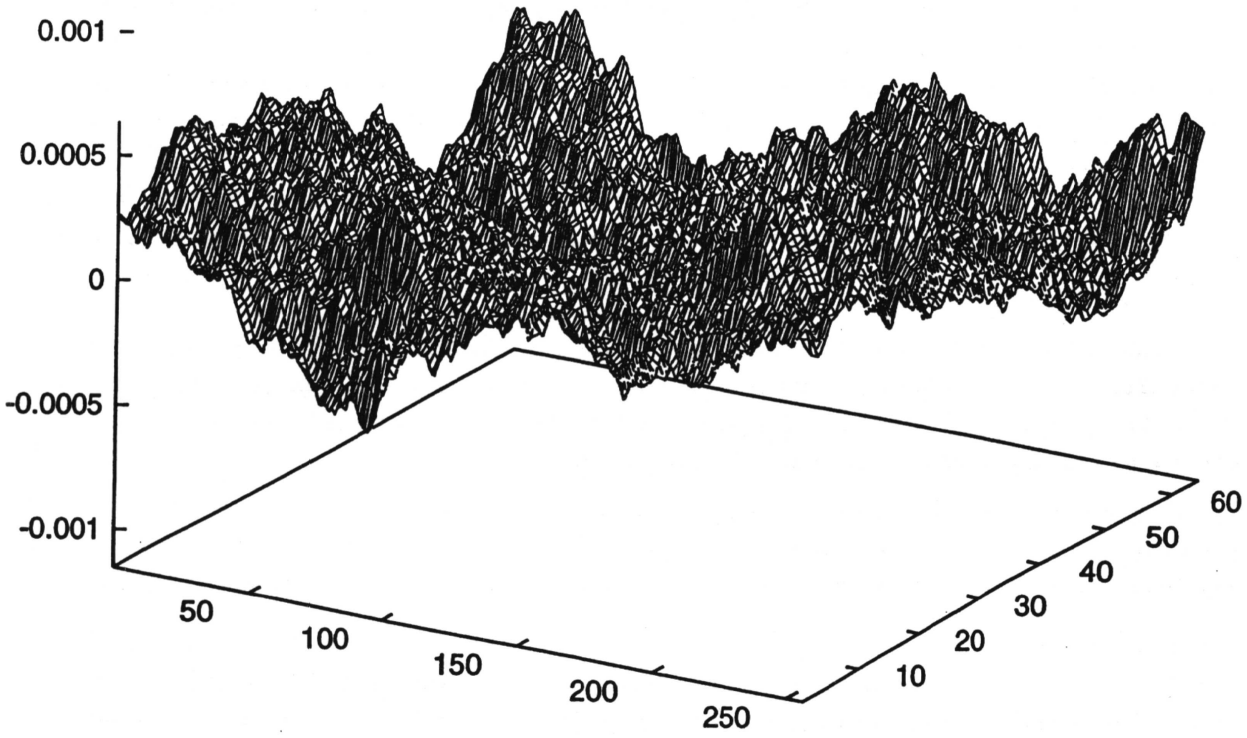

Figure 7. Fractional Brownian Surface with $H = 0.5$.

Turning from the geometrical to the dynamical complexity, and going beyond the characteristic power laws previously studied, the stick–slip behavior is sure retained one of the most impressive feature of the seismic phenomenology.

The idea is that in periods between ruptures (stick) stress is accumulated due to continuing tectonic movement until a certain threshold is overcome resulting in a sudden slip, and reducing the built–up stress. Blockages or frictional resistance is overcome. In this way Brace and Byerlee [46] defined earthquakes as recurring slip instabilities on preexisting faults, namely stick–slip phenomena.

One of the first model which simulated this mechanism is the Burridge–Knopoff model previously treated.

In the SAM model perspective sticking is conceptually a configuration with opposite asperities that stop the relative translational tectonic motion after their collision. After a certain quiescience time a threshold is reached and abruptly the weaker asperity breaks allowing the system to slip. Asperities correspond therefore in turn to zones with higher than usual frictional resistance where stress is accumulated, and to regions with an exceptionally high moment release and stress drop.

As in the last section, we now incorporate some rules in the model to extend the geometrical to a simulation of the dynamical complexity in order to investigate their effect on the characteristic power law behavior.

The model steps comprised the following dynamical rules:

(1) Generating, as initial condition at the synthetic time $t = 0$, a 2D fractal fault by placing two discretized fB surfaces on parallel grid supports at an infinite distance:

$$S_H^{\inf}(i,j) \qquad i = 1, 2, \ldots, L_{\inf} \qquad j = 1, 2, \ldots, w$$
$$S_H^{\sup}(i,j) \qquad i = 1, 2, \ldots, L_{\sup} \qquad j = 1, 2, \ldots, w$$

where w is the fault width and $L_{\inf}, L_{\sup}$ are respectively the lengths of the inferior and superior segments of the fault.
We have studied two sets with different fault dimensions:
Set a) $w = 32, L_{\inf} = 32, L_{\sup} = 512$.
Set b) $w = 64, L_{\inf} = 256, L_{\sup} = 1024$.
For each set we have produced realizations with three different values of roughness:

$$H = 0.3, \quad 0.5, \quad 0.7.$$

Figure 7 depicts a realization of a fB surface with $w = 64, L = 256$ and $H = 0.5$.

(2) Placing the two surfaces into contact at the point where the height difference is minimal:

$$S_H^{\sup}(i,j) = {}^{\text{old}}S_H^{\sup}(i,j) + \max_{\substack{i=1,\ldots,L_{\inf} \\ j=1,\ldots,w}} \left(S_H^{\inf}(i,j) - {}^{\text{old}}S_H^{\sup}(i,j) \right),$$

$i = 1, 2, \ldots, L_{\sup},\ j = 1, 2, \ldots, w$.
This rule simulates the action of a force perpendicular to the slip direction which presses the fault surfaces against each other.

(3) Translating the superior surface parallel to the i–axis of slip one unit grid spacing (equal to the distance between two nearest point in the grid) when the synthetic time progresses from t to $t + 1$:

$$S_H^{\sup}(i,j) = S_H^{\sup}(i+1,j) \qquad i = 1, 2, \ldots L_{\sup} - 1 \qquad j = 1, 2, \ldots, w$$
$$S_H^{\sup}(L_{\sup},j) = k \qquad\qquad j = 1, 2, \ldots, w$$

where $k \gg \max S_H^{\sup}$ is a constant.
With these rules the choice $L_{\sup} > L_{\inf}$ results in a well–defined procedure.

(4) Repeating from step 2., if there is not any overlap, and until the condition of overlap is obtained, i.e., until there is at least a site (i, j) with

$$S_H^{\sup}(i,j) < S_H^{\inf}(i,j).$$

The condition of overlap represents the configuration with asperities colliding and obstructing the tectonic translational movement (stick–period). There is a non zero probability to obtain an overlap condition contemporaneously in sites far one from another in the grid.

(5) Calculating the quiescence time, deciding which is the weakest overlap site from which the earthquake fracture will start, and which of the two asperities will break in that site. Making the abrupt slip start after having calculated its length. During the slip, which is retained instantaneous, all the asperities which obstruct the sliding mechanism are destroyed. At the end of the slip a condition of no–overlapping in any points is obtained and the mechanism can be restarted from point 2..

In this procedure we made use of the following definitions:

(1) A synthetic earthquake is the result of the break of an asperity at the contact where two points on the mesh share the same position. We then assume that the smaller asperity breaks (if the two asperities have the same linear dimension, we have chosen to break one of them at random). The resultant fracture is itself simulated as a fB surface with the same Hurst parameter H, and extends until it crosses again with the principal fault surface, or until it reaches the bounds site with coordinates so that $i = 1, i = L_{\text{inf}}, j = 1$ or $j = w$.
(2) The linear dimension of the asperity is the distance between the contact point and that point in the slip direction (i–axis) obtained from the intersection of the asperity with an horizontal plane at the contact height.
(3) The weakest overlap site, in a configuration with more than one overlapping point, is that site whose smaller asperity has the minimum linear dimension. Associated to this point there is the "main asperity", i.e. that one from which the first crack will start giving rise to the entire rupture.
(4) The waiting time until next earthquake is a delay in the time–stepping routine equal to the linear dimension of the smaller main asperity before the breaking mechanism. In this way the model intrinsically reproduces the stick–slip property.
(5) The energy W (or equivalently the seismic moment M) of an earthquake is proportional to the total rupture area A and to the mean slip d over that area ($M = Ad$). For the purpose of evaluating the model results we define the model seismic moment with slip $d =$ (linear dimension of the smaller main asperity), $A =$(total area comprehending all the rupture points, i.e. all those sites of the superimposition grid ($w \times L_{\text{inf}}$) whose heights in the superior or inferior surfaces have changed because of the rupture).
(6) The hypocenter is that point where the rupture initiates at the main asperity.

As in the 1D SAM version, and according to the same argumentation previously adduced, we have supposed the wear material not to interact in the slipping mechanism as if the region between the two fault surfaces could be retained empty.

All the preceeding rules and definitions have been chosen with the aim of coming to a sort of compromise between the great complexity of the phenomena which we want to reproduce, and the pratical difficulties due to the translation of the ideas in algorithms which could allow the program to be controlled and to work in a reasonable time.

Obviously it is possible to extend the model to more realistic generalizations of the breaking and slipping mechanism. As an example, hypothetically it would be interesting to study the stress redistribution in the medium to establish the position of the crack starting point with respect to the point of application of pressure, or to determine the total slip of an event through a frictional cumulative braking mechanism due to the opposite asperities met during the sliding period.

The relatively more simplified dynamical rules above reported allowed us to generate synthetic earthquakes from the numerical evolution of the model. To function as a viable model for studying earthquake statistics, the 2D SAM case must evidence specific general properties of the seismic phenomena. Most prominently we have studied the Gutenberg–Richter (GR) law and the distribution of hypocenters set both in space and in time.

3.1. **Gutenberg–Richter Law.**

We have focused our attention on the GR law. Experimentally the size distribution statistics for earthquake does not perfectly agree with the standard GR power law: large earthquakes do not belong to the same fractal set of small ones. The fractal set has broken in two subsets, in which both small and large events have power law size distributions but with different exponents. The introduction of a characteristic length w, such as the fault's width in our dynamical rules, representing the thickness of the brittle part of the Earth lithosphere (the schizosphere), induces and so justifies the presence of two fractal dimensions, one for small and one for large earthquakes, with rupture dimensions respectively smaller and larger than the schizosphere thickness w [23].

In fact the dimensionality of earthquakes changes at the length scale w: a small rupture event has two freedom degrees to propagate, and so represents a rupture in an unbounded elastic brittle solid, whereas, once an earthquake becomes large it can propagate further in the horizontal direction since the vertical dimension is bounded between the Earth surface and the ductile region. This helps to explain why faults can reach lengths up to 1000 km while their widths w have values of some tens of kilometers.

In particular, to better understand the relationship between the schizosphere and the rupture events, the depth w corresponds to a critical value of temperature T_C (≈ 300°C for continental granitic rock types) at which ductility begins to dominate the deformation since there is a transition from an unstable velocity–weakening friction ($T < T_C$, stick–slip) to a stable velocity–strengthening friction ($T > T_C$).

Turning to our numerical results, we have studied the synthetic GR statistics from the evolution of the 2D SAM model for three different kind of fault roughness ($H = 0.3, 0.5, 0.7$) and for two different sizes of the fault surfaces ($w \times l = 32 \times 32, 64 \times 256$).

Thanks to a device, which has allowed us not to exhaust the superior fault surface because of its sliding movement, we have produced many realizations each with $N = 1000$ synthetic eartquakes. We have then studied the GR statistics for each set of N earthquakes.

The synthetic data present a good power law behavior with a deviation similar to that already shown in figure 2, relative to the 1D version of the model, for those earthquakes with the smallest energy, which are overestimated: in the contact routine between the two fault surfaces there is a greater probability that only the extreme tops of the asperities will collide giving consequently rise to a great number of small events (as if the normal forces, which push the two surfaces one against the other in the direction perpendicular to slip, were too weak). The ruptures associated to these earthquakes have difficulty in escaping from the tops of the asperities and so do not change in a considerable way the configuration of the fault. We have so decided to cut these data (with $M < 20$) from our following evaluation, associating them to those real events with an energy lower than the minimum detection threshold.

On the contrary, as about large events, there is a noisy spreading in the data points, due to their low statistics, which for $N = 1000$ does not allow us to detect the two fractal dimensions inferred from the characteristic width of the fault.

We report now some averaged values of exponents d of the GR law from many different samples of numerical simulations with H and the fault size varying.

Since $N(M) \propto M^{-d}$, the relationship between d and the *b–value* is $d = b/c+1$ with $c \cong 1.5$ [32].

In table 1 the two fractal dimensions d_1 and d_2, respectively for small and large energy events, are showed for a fault system with surface $w \times l = 32 \times 32$ and number of earthquake $N = 15000$ for each of the three value of H in the interval $[0.3, 0.7]$. In the last line it is also possible to see the values relative to the totality of earthquakes relative to a distribution of faults with different roughnesses.

H	N	d_1	d_2
0.3	15000	1.249 ± 0.033	1.980 ± 0.229
0.5	15000	1.178 ± 0.026	1.720 ± 0.231
0.7	15000	1.128 ± 0.030	1.673 ± 0.242
$0.3 + 0.5 + 0.7$	45000	1.184 ± 0.019	1.770 ± 0.128

TABLE 1. $w \times l = 32 \times 32$.

In table 2 is reported a comparison between the two systems with different fault surface for $N = 5000$ and with H varying. Because of the lower statistics (with respect to $N = 15000$ of the last table), which causes the spreading of those data points relative to large energy events, the two exponents cannot be distinguished any more. The d values reported have been so calculated in such a way to be more representative of earthquakes with small and intermediate energies.

In table 3 the two exponents d_1 and d_2 are based on data points coming from faults with both sizes while H varying. Each of the three sets with $N = 20000$ earthquakes is composed

Size	H	N	d
64×256	0.3	5000	1.218 ± 0.043
64×256	0.5	5000	1.126 ± 0.042
64×256	0.7	5000	1.071 ± 0.040
32×32	0.3	5000	1.405 ± 0.052
32×32	0.5	5000	1.335 ± 0.057
32×32	0.7	5000	1.253 ± 0.048

Table 2. $w \times l = 32 \times 32$.

by $N = 15000$ events relative to faults systems with area $w \times l = 32 \times 32$, and $N = 5000$ events coming from faults such that $w \times l = 64 \times 256$.

H	N	d_1	d_2
0.3	20000	1.239 ± 0.034	1.732 ± 0.068
0.5	20000	1.141 ± 0.026	1.609 ± 0.077
0.7	20000	1.102 ± 0.020	1.344 ± 0.071
$0.3 + 0.5 + 0.7$	60000	1.162 ± 0.015	1.584 ± 0.043

Table 3. $(w \times l = 32 \times 32) + (w \times l = 64 \times 256)$.

Note how, as in the 1D SAM version, the exponent of the GR is a decreasing function of H (see last section for an explanation).

The real novelty is that the fractal dimension d depends on the size of the fractal surface too. In particular we can give the simple following interpretation. In the case with grid size 32×32, we deal with a fault with a square shape which is so bounded in its horizontal length l at the same way as in its width w corresponding to the schizosphere thickness. Consequently the large ruptures have difficulty in propagating since they find bounds in each direction, increasing in this way the probability of obtaining small events. In the second case with grid size 64×256 the length of the fault has been increased with respect to the width. The fault has a more real rectangular shape, and large ruptures have a way out in the horizontal direction increasing their probability to happen; consequently the GR exponent d decreases with respect to the 32×32 value while H being the same. In reality also the horizontal direction is bounded; however the size difference with respect to the width allow the above mentioned effect.

This argumentation perfectly agrees with the data obtained in table 2 where, for each choice of H, the exponents d relative to the larger grid size have always values smaller than those ones coming from the smaller grid size. In the same optics it is now understandable how, for each choice of H, the d_1 in table 3 are intermediate values between the larger d_1 values of table 1 and the smaller d values relative to $w \times l = 64 \times 256$ of table 2.

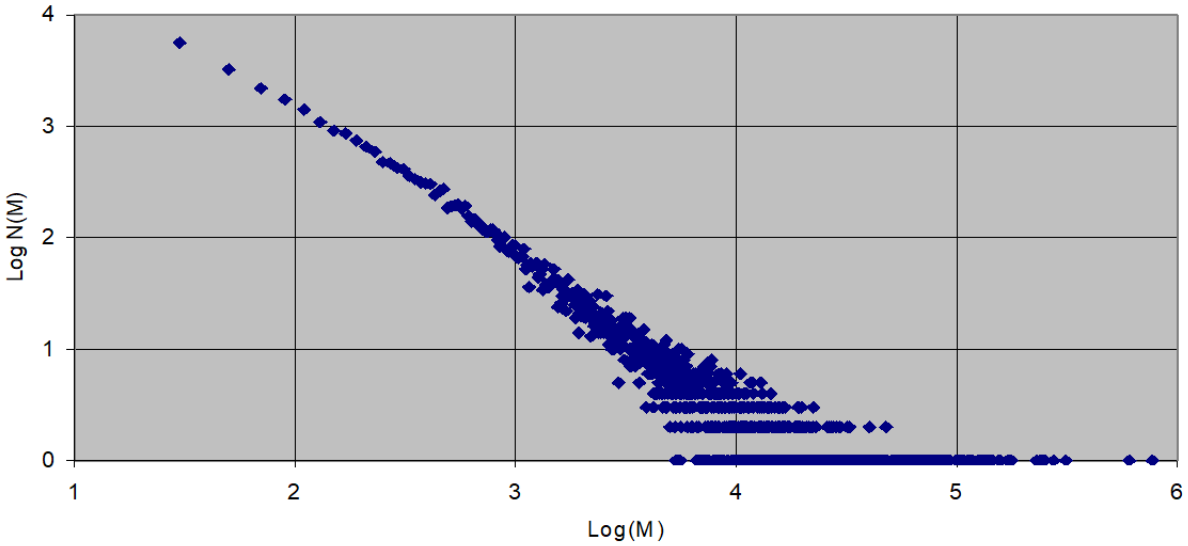

FIGURE 8. Non cumulative Gutenberg–Richter law with two scaling exponents from 2D SAM model.

Note besides how, according to experimental data, d_2 is always greater than d_1, and how the values obtained for the fractal dimension between the mimimum $d = 1.07$ and the maximum $d_2 = 1.98$ correspond to values of b in the interval $[0.11, 1.47]$ in good agreement with experimentally measures data.

In figure 8, in a log–log plot, it is reported the graph representing the GR power law summing the data from the totality of $N = 60000$ synthetic earthquakes (less those ones which have been cutted because $M < 20$) produced in different faults systems with different grid sizes and roughness parameters H.

Though the effect of the breaking of the fractal set in two subsets with two scaling exponents is damped from the existence of the even if larger horizontal bound, the presence of the two exponents ($d = 1.16$ for small events and $d = 1.58$ for large ones) can be easily detected.

Note that the critical seismic moment level that separates the two different fractal subsets ($\log M' = 2.67$ in figure 8; $\log M' = 2.66 \pm 0.06$ is the average of all the considered samples) depends on the local tectonic configurations. Theoretically in faults with a width w and unbounded horizontal dimension, approximating a critical earthquake as a rupture surface with typical dimension equal just to w, we can simply derive a relationship between the critical seismic moment M' which separates small and large events and the schizosphere thickness w:

$$M' = \frac{16}{7} \Delta\sigma \cdot w^3$$

with $\Delta\sigma$ within the range $0.1 - -10$ MPa being the stress drop [23].

Earthquakes with a seismic moment larger than M' can only propagate increasing their horizontal length L since their width w becomes fixed. Their seismic moment becomes so proportional to the length squared instead of length cubed. It would be interesting to produce numerical realizations from the 2D SAM model for different values of w (with horizontal fault lengths $l \gg w$) to check the last equation.

Globally, in contrast with the universality of the *b–value* stated by SOC models, we have so confirmed some peculiarities present in the 1D SAM version, and found a new characteristic too: in our interpretation the fluctuations of the b exponent are not only statistical but are due to the structural and geometrical properties of the different faults. In particular the *b–value* seems to be dependent on the roughness, through the Hurst parameter, and on the characteristic dimensions of the fault surfaces fixed by some structural bounds both in their width and in their length.

3.2. **Hypocenters in Space and Time.**

Box–counting method applied to synthetic hypocenters, obtained from the numerical evolution of the 2D SAM model, stresses that they comprise a spatial fractal set. The fractal dimension D_s is strongly dependent on the number N of earthquakes per realization, and is in particular an increasing function of N with

$$\lim_{N\to\infty} D_s(N) = 2.$$

The limit $D_s = 2$ corresponds to an homogeneous filled plane in discretized case where each site of the grid has been the hypocenter of at least one of the infinite events happened in the grid. In this perspective we have for example obtained that in a grid 32×32 with $H = 0.3$ the average value $D_s(N = 1000) = 1.74$ and $D_s(N = 2000) = 1.82$.

The spatial fractal dimension seems also to be a decreasing function of H. For a fault size 32×32 with $N = 1000$ we have in fact obtained that $D_s = 1.74, 1.66, 1.58$ respectively for $H = 0.3, 0.5, 0.7$.

This intuitively means that under the same N for a more jagged fault surface, i.e. for low H values, because of the plenty of small asperities there are much more different sites in the grid where collisions happen and the discretized plane fills up with a higher velocity in function of N.

Instead, the temporal study obtained by evaluating the set of events in time with the box–counting and the Grassberger–Procaccia method for the correlation dimension gives an exponent indicating a uniformly random distribution without fractal clustering. This is in contrast to the clusterization of events measured in some experimental works [47]. We think that our result is strongly affected by there being a large probability that only the extreme tops of the asperities collide giving rise to a many waiting times of short lengths. The great majority of events happens in this way with time intervals random distributed between a restricted range of short values.

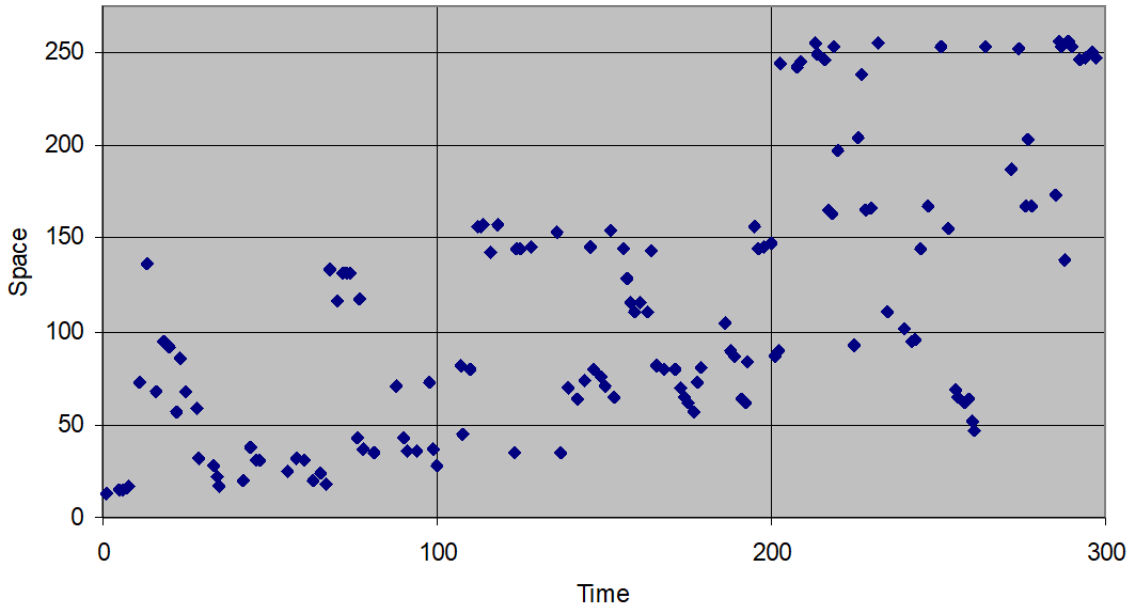

FIGURE 9. 2D SAM results for the space–time distribution of epicenters.

We have finally studied the space–time distribution of hypocenters. In figure 9 is reported the projections (i.e. epicenters) on the i–coordinate of those hypocenters obtained in a certain temporal window for a numerical simulation with $H = 0.5$ and $w \times l = 64 \times 256$. So as in section 2 for the 1D version of the model, also in 2D there is some evidence of the migration of the seismic events, i.e. a correlation of earthquakes in time in form of oblique lines which join the epicenters.

In particular a set of points with a straight line shape represents the earthquakes caused by an asperity belonging to the superior fault surface which collide repeatedly with opposite smaller asperities in its motion in the negative sense of the i–axis. Because of the disappearence of the configuration with constant translating velocity, due to the new waiting time mechanism, the oblique lines relative to figure 9 are much less marked with respect to the 1D SAM case (see figure 5a), and their slope is no more at 45 degrees. As far as additional considerations are concerned, refer to the analogue argumentations of section 2.

4. CONCLUSIONS

In this work we have moved in two directions: the first was to improve the knowledge of the 1D SAM model with breaking mechanism, which had been studied before only for the treatment of the Omori law [21], testing it through other general statistical properties; second, we have extended the model in 2D reproducing a more complex stick–slip dynamics.

Globally, the model has shown interesting results well reproducing some seismic general properties which cannot be discriminated from statistics produced by a study of empirical earthquakes, such as the Gutenberg–Richter (GR) law, a not trivial distribution of epicenters and hypocenters in space and in time, and a fractal distribution of wear material, and strengthening the idea that critical behavior in seismic phenomenology could be directly generated by the fractal geometrical complexity of the faults. In our interpretation the local accumulation of stress is at the very origin of the earthquakes.

The question we have focused on has concerned the research of the causes and particularly the manners which have allowed the SAM model statistics to be similar to statistics for earthquakes distribution in space and time. Being conscious that two different phenomena can produce the same kind of response when evaluated in a certain way, and that models results cannot prove or disprove internal either external hypotheses, we have side by side used SOC systems as comparison tool with SAM interpretation. More specifically, the controversy about the universality or not of the *b–value* in the GR law has represented a central matter of debate. An improved understanding of this fundamental parameter, especially its physical basis, has in fact direct implications for the earthquake generation processes and earthquake prediction research.

Interesting is, in this optics, the property by which, in the SAM model perspective, the fluctuations of the *b–value* are not only statistical but can be reduced to difference in the faults roughness, and to their varying dimensions fixed by some structural bounds. The last characteristic seem to be at the basis of the presence of two different scaling exponents for small and large events.

References

[1] S. Das, B. V. Kostrov, J. Geophys. Res. B 88, 4277 (1983).
[2] E. C. Robertson, Min. Eng. 35, 1426 (1983).
[3] B. Gutenberg, C. F. Richter, Ann. Geophys. 9, 1 (1956).
[4] F. Omori, Rep. Earth. Inv. Comm. 2, 103 (1894); T. Utsu, J. Fac. Sci. Hokkaido Univ. Serv. VII 3, 197 (1970).
[5] K.Ito, M. Matsuzaki, J. Geophys. Res. B 95, 6853 (1990).
[6] C. G. Sammis, R. H. Osborne, J. L. Anderson, M. Banerdt, P. White, Pageoph. 123, 53 (1986); C. G. Sammis, R. Biegel, Pageoph. 131, 255 (1989).
[7] Y. Y. Kagan, L. Knopoff, Geophys. J. R. Astron. Soc. 62, 303 (1980); T. Ouchi, T. Uekawa, Phys. Earth Planet. Inter. 44, 211 (1986); V. De Rubeis, P. Dimitriu, E. Papadimitriou, P. Tosi, Geophys. Res. Lett. 20, 1911 (1993).
[8] R. Burridge, L. Knopoff, Bull. Seismol. Soc. Am. 57, 341 (1967).
[9] P. Bak, C. Tang, K. Wiesenfeld, Phys. Rev. Lett. 59, 381 (1987); Phys. Rev. A 38, 364 (1988).
[10] D. Sornette, in: *Spontaneous Formation of Space–Time Structures and Criticality*, T. Riste, D. Sherrington eds., Kluwer Acad. Publ., 1991, pp. 57–106; I. Main, Rev. of Geophys. 34, 433 (1996).
[11] J. M. Carlson, J. S. Langer, Phys. Rev. Lett. 62, 2632 (1989); Phys. Rev. A. 40, 6470 (1989).
[12] A. Vespignani, S. Zapperi, L. Pietronero, Phys. Rev. E 51, 1711 (1995).
[13] P. Bak, C. Tang, J. Geophys. Res. 94, 15 635 (1989); H. Nakanishi, Phys. Rev. A 43, 6613 (1991); H. Takayasu, M. Matsuzaki, Phys. Rev. Lett. A 131, 244 (1988).

[14] Z. Olami, H. J. S. Feder, K. Christensen, Phys. Rev. Lett. 68, 1244 (1992); K. Christensen, Z. Olami, J. Geophys. Res. 97, 8729 (1992).
[15] A. Crisanti, M. H. Jensen, A. Vulpiani, G. Paladin, Phys. Rev. A 46, R7363 (1993).
[16] P. G. Okubo, K. Aki, J. Geophys. Res. 92, 345 (1987); K. Aki, Tectonophys. 211, 1 (1992).
[17] R. Madariaga, J. Geophys. Res. 84, 2243 (1979); J. Rudnicki, H. Kanamori, J. Geophys. Res. 86, 1785 (1981); A. Mc Garr, J. Geophys. Res. 86, 3901 (1981); T. Lay, H. Kanamori, L. Ruff, Earthq. Predict. Res. 1, 3 (1982).
[18] R. Wu, K. Aki, Pageoph. 131, 805 (1985); S. R. Brown, C. H. Scholz, J. Geophys. Res. 90, 12 575 (1985); W. L. Power, T. E. Tullis, S. R. Brown, G. N. Boitnott, C. H. Scholz, Geophys. Res. Lett. 14, 29 (1987); B. L. Cox, J. S. Y. Wang, Fractals 1, 87 (1993); J. Schmittbuhl, J. Geophys. Res. 100, 5953 (1995).
[19] B. Mandelbrot, *The Fractal Geometry of Nature*, Freeman, New York, 1983.
[20] V. De Rubeis, R. Hallgass, V. Loreto, G. Paladin, L. Pietronero, P. Tosi, Phys. Rev. Lett. 76, 2599 (1996).
[21] R. Hallgass, V. Loreto, O. Mazzella, G. Paladin, L. Pietronero, Phys. Rev. E 56, 1346 (1997).
[22] J. Delsemme, A. T. Smith, Pageoph. 117, 1271 (1979).
[23] C. H. Scholz, in: *Spontaneous Formation of Space–Time Structures, Criticality*, T. Riste, D. Sherrington eds., Kluwer Acad. Publ., 1991, pp. 41–56 ; Bull. Seismol. Soc. Am. 87, 1074 (1997).
[24] C. H. Scholz, *The mechanics of Earthquakes and Faulting*, Cambridge Univ. Press, Cambridge, 1990, pp. 45, 217.
[25] J. M. Kemeny, R. M. Hagaman, Pageoph. 138, 549 (1992).
[26] L. J. Ruff, Tectonophys. 211, 61 (1992).
[27] R. F. Voss, Physica D 38, 362 (1989).
[28] H. E. Hurst, R. P. Black, Y. Simaika, *Long–Term Storage: An Experimental Study*, Constable, London, 1965; J. Feder, in: *Spontaneous Formation of Space–Time Structures and Criticality*, T. Riste, D. Sherrington eds., Kluwer Acad. Publ., 1991, pp. 113–135.
[29] R. F. Voss, in: *The Science of Fractal Images*, H.–O. Peitgen, D. Saupe eds., Springer, Berlin, 1988, Ch.2, p.108.
[30] H. J. Hermann, G. Mantica, D. Bessis, Phys. Rev. Lett. 65, 3223 (1990).
[31] J. Huang, D. L. Turcotte, Earth Planet. Sci. Lett. 91, 223 (1988).
[32] H. Kanamori, D. L. Anderson, Bull. Seismol. Soc. Am. 65, 1073 (1975); T. C. Hanks, H. Kanamori, Geophys. Res. 84, 2348 (1979).
[33] S. Wesnousky, C. Scholz, K. Schimazaki, J. Geophys. Res. 88, 9331 (1983).
[34] K. Aki, J. Geophys. Res. 84, 1349 (1987).
[35] H. Xie, in: *Fractals in Rock Mechanics*, Geomechanics Res. series n.1, A.A. Balkema, Rotterdam, 1993, p. 409.
[36] K. Mogi, Tectonophys. 5, 35 (1967).
[37] C. H. Scholz, Bull. Seismol. Soc. Am. 58, 399 (1968); J. Weeks et al., Bull. Seismol. Soc. Am. 68, 333 (1978).
[38] L. W. Teufel, J. M. Logan, Pageoph. 116, 840 (1978); C. H. Scholz, *The mechanics of Earthquakes and Faulting*, Cambridge Univ. Press, Cambridge, 1990, pp. 46–48.
[39] D. L. Turcotte, Fractals and Chaos in Geology and Geophysics (Cambridge Univ. Press, Cambridge, 1992), p. 29.
[40] R. Biegel, C. G. Sammis, J. H. Dietrich, J. Struct. Geol. 11, 827 (1989).
[41] S. Schlien, M. N. Toksoz, Bull. Seism. Soc. Am. 60, 1765 (1970).
[42] K. Mogi, Bull. Earthquake Res. Inst. 46, 53 (1968); J. A. Kelleher, J. Geophys. Res. 75, 5745 (1970); M. D. Wood, S. S. Allen, Nature 244, 213 (1973).
[43] C. H. Scholz, Nature 267, 121 (1977); *The mechanics of Earthquakes and Faulting*, Cambridge Univ. Press, Cambridge, 1990, pp. 210–216.

[44] O. Mazzella, *Modelli Stocastici per l'Invarianza di Scala nell'Attività Sismica*, Laurea Thesis, Como University (1996), pp. 93–99.
[45] W. L. Power, T. E. Tullis, S. R. Brown, G. N. Boitnott, C. H. Scholz, Geophys. Res. Lett. 14, 29 (1987); C. H. Scholz, *The mechanics of Earthquakes and Faulting*, Cambridge Univ. Press, Cambridge, 1990, pp. 146–147.
[46] W. F. Brace, J. D. Byerlee, Science 153, 990 (1966); J. D. Byerlee, W. F. Brace, J. Geophys. Res. 73, 6031 (1968).
[47] M. A. Sadovskiy, T. V. Golubeva, V. F. Pisarenko, M. G. Shnirman, Phys. Solid Earth 20, 87 (1985); R. F. Smalley, J. L. Chatelain, D. L. Turcotte, R. Prévot, Bull. Seism. Soc. Am. 77, 1368 (1987).